The mechanical and thermal structure of Mercury's early lithosphere

Thomas R. Watters,[1] Richard A. Schultz,[2] Mark S. Robinson,[3] and Anthony C. Cook[1]

Received 1 November 2001; revised 15 February 2002; accepted 22 February 2002; published 14 June 2002.

[1] Insight into the mechanical and thermal structure of Mercury's early lithosphere has been obtained from forward modeling of the largest lobate scarp known on the planet. Our modeling indicates the structure overlies a thrust fault that extends deep into Mercury's lithosphere. The best-fitting fault parameters are a depth of faulting of 35 to 40 km, a fault dip of 30° to 35°, and a displacement of ~2 km. The Discovery Rupes thrust fault probably cut the entire elastic and seismogenic lithosphere when it formed (~4.0 Gyr ago). On Earth, the maximum depth of faulting is thermally controlled. Assuming the limiting isotherm for Mercury's crust is ~300° to 600°C and it occurred at a depth of ~40 km, the corresponding heat flux at the time of faulting was ~10 to 43 mW m^{-2}. This is less than old terrestrial oceanic lithosphere but greater than the present heat flux on the Moon. *INDEX TERMS:* 5475 Planetology: Solid Surface Planets: Tectonics (8149); 6235 Planetology: Solar System Objects: Mercury; 5464 Planetology: Solid Surface Planets: Remote sensing; 5430 Planetology: Solid Surface Planets: Interiors (8147); 5460 Planetology: Solid Surface Planets: Physical properties of materials

1. Introduction

[2] One of the most remarkable discoveries of the Mariner 10 mission was the widespread occurrence of landforms described as lobate scarps that reflect significant crustal deformation [*Strom et al.*, 1975; *Cordell and Strom*, 1977; *Melosh and McKinnon*, 1988]. Lobate scarps occur as linear or arcuate segments, and vary in length from tens to hundreds of kilometers [*Strom et al.*, 1975; *Cordell and Strom*, 1977]. In cross-section, these landforms generally consist of a steeply sloping scarp face and a gently sloping back scarp. The maximum relief of lobate scarps varies from hundreds to over a thousand meters [*Watters et al.*, 1998]. Based on morphology and offsets in crater wall and floor materials, lobate scarps are interpreted to be the surface expression of thrust faults [*Strom et al.*, 1975; *Cordell and Strom*, 1977; *Melosh and McKinnon*, 1988; *Watters et al.*, 1998, 2001]. Thrust faulting is thought to have initiated after the period of heavy bombardment (~4.0 Gyr ago), post-dating the emplacement of the intercrater plains [*Melosh and McKinnon*, 1988]. Discovery Rupes (53°S, 37°W) is the largest lobate scarp (>500 km in length) on the hemisphere imaged by Mariner 10 [*Strom et al.*, 1975; *Cordell and Strom*, 1977] (Figure 1). Stereo measurements and photoclinometry show this structure has a maximum relief of ~1.5 km [*Watters et al.*, 1998, 2001] and provide a detailed look at its morphometry. Although the thrust fault kinematic model is widely accepted, the fault geometry, fault-plane dip, and depth of faulting are unconstrained. We test the validity of the thrust fault origin proposed for lobate scarps by forward mechanical modeling constrained by topography across Discovery Rupes.

[3] Estimates of the maximum thickness of Mercury's crust range from to 200 to 300 km [*Schubert et al.*, 1988; *Spohn*, 1991; *Anderson et al.*, 1996; *Nimmo*, 2002]. The effective elastic thickness of Mercury's lithosphere is thought to be on the order of 100 km or more at present, having increased with time as the planet cooled and its heat flow declined [*Melosh and McKinnon*, 1988]. Although Mercury's early lithosphere was probably thinner, there is no evidence to support this hypothesis. Mechanical modeling of the Discovery Rupes thrust fault allows us to constrain the maximum depth of faulting which provides insight into the structure of Mercury's lithosphere around the end of the period of heavy bombardment.

2. Topography and Analysis

[4] Topographic data for Mercury are being derived from digital stereoanalysis [*Watters et al.*, 1998, 2001; *Cook and Robinson*, 2000], using updated Mariner 10 camera orientations [*Robinson et al.*, 1999]. Topography is obtained using an automated stereo matching process that finds corresponding points in stereo images using a correlation patch of a given radius [e.g., *Day et al.*, 1992]. As patch size is increased, the derived topography is smoothed and the relief of short wavelength topographic features is reduced [*Cook et al.*, 1998; *Wilkison et al.*, 2001]. Combining digital elevation models (DEMs) derived from different patch radii preserves the short wavelength topography while reducing noise in the long wavelength topography. From the Mariner 10 images, DEMs with a typical grid spacing of 2 km/pixel can be produced. The southern half of Discovery Rupes is covered by Mariner 10 stereo pairs (Figure 1). The relative height accuracy of the derived DEM is estimated to be about ±100 m in areas of good stereo matching (i.e., maximal image texture) based on a comparison of the average maximum relief determined independently from photoclinometry [*Watters et al.*, 1998]. The greatest relief on Discovery Rupes occurs just south of Rameau crater (60 km in diameter) (Figure 1) averaging 1.3 km (range 1.1 to 1.5 km) over a 12 km section (profiles taken at 2 km intervals on either side of profile A-A′ shown in Figure 1). The topographic data reveal a broad, shallow trough roughly 90 km west of the base of the scarp (Figures 1 and 2). The trough is about 40 km wide and several hundred meters deep, and roughly parallels the scarp. The extent of the trough is visible in the DEM (Figure 1). We interpret this trough to be evidence of a trailing syncline and the distance between it and the surface break defines the cross-strike dimension of the upper plate of the thrust fault.

[5] The presence of a topographic depression in the back scarp area is not unique to Discovery Rupes. Preliminary analysis of the topography across Adventure Rupes, another mercurian large-scale lobate scarp, indicates that it also has a parallel trough about 80 km from the base of the scarp. A shallow topographic depression is observed behind the scarp face of an analogous lobate scarp on Mars called Amenthes Rupes [*Watters et al.*, 2000; *Schultz and Watters*, 2001]. Surface breaking terrestrial thrust fault scarps also have similar

[1]Center for Earth and Planetary Studies, National Air and Space Museum, Smithsonian Institution, Washington, DC, USA.
[2]Department of Geological Sciences, Mackay School of Mines, University of Nevada, Reno, USA.
[3]Department of Geological Sciences, Northwestern University, Evanston, Illinois, USA.

0094-8276/02/2001GL014308$05.00

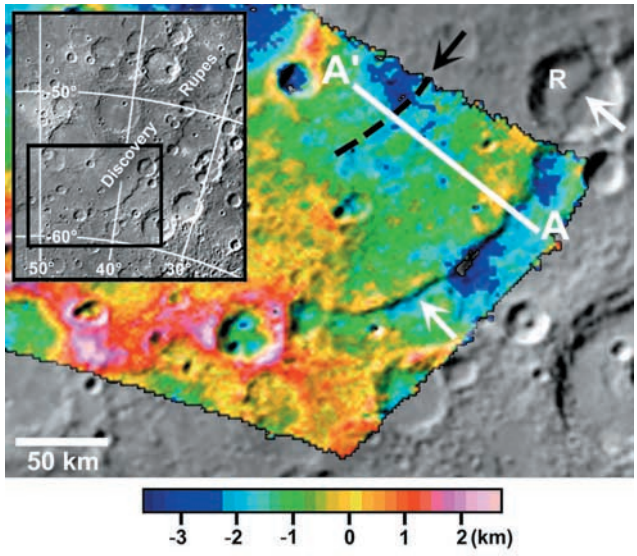

Figure 1. Color-coded DEM generated using Mariner 10 stereo pair 27399 (~240 m/pixel) and 166613 (~670 m/pixel), overlaid on an image mosaic. The DEM was generated by combining topography derived from three correlation patch radii (5, 7, and 9 pixels). The inset shows the location of Discovery Rupes and the area shown in the figure. The white line indicates the location of the topographic profile (A-A′) across Discovery Rupes (white arrows) shown in Figures 2 and 3. The black arrow and dashed line shows the location of a broad, shallow depression. Rameau crater is indicated by an R on the image. Elevations are relative to 2439.0 km reference sphere.

topographic expressions to these planetary lobate scarps [see *King et al.*, 1988; *Taboada et al.*, 1993].

3. Mechanical Model

[6] The boundary element dislocation program Coulomb 2.0 [*King et al.*, 1988; *Toda et al.*, 1998] was used to model the surface displacements associated with the Discovery Rupes thrust fault. Forward mechanical dislocation modeling provides a good approximation to the topography within a relatively narrow range of parameters [*Cohen*, 1999; *Schultz and Watters*, 2001]. This method has been successfully applied to terrestrial faults where the displacement is known [e.g., *King et al.*, 1988; *Bilham and King*, 1989; *Toda et al.*, 1993]. The sense of slip and the amount of displacement on the fault is specified, and the resulting stresses and material displacements are determined [*Okada*, 1992]. Model parameters are constrained by the agreement between the predicted and observed topography. The fault surface is approximated by a rectangular plane having a fault-plane dip angle θ, and vertical depth of faulting T (Figure 2). The lower tip of the thrust fault is placed below the trailing syncline and its upper tip at the surface break. The initial magnitude of displacement D is estimated from the height of the scarp adjacent to the surface break.

[7] Mercury's lithosphere is modeled using an elastic halfspace. It is assumed that the strength of Mercury's lithosphere is in a seismogenic (brittle) layer that extends to a weaker lower lithosphere [see *Scholz*, 1998; *Maggi et al.*, 2000]. Although an elastic halfspace does not account for the effects of a weaker lower lithosphere, results obtained modeling deeply rooted terrestrial thrust faults [e.g., *Stein et al.*, 1994] suggest it is a reasonable approximation when its frictional stability (i.e., faulting) is considered. An elastic modulus E of 80 GPa and Poisson's ratio ν of 0.25 are assumed for Mercury's lithosphere, comparable to values for terrestrial lithosphere [e.g., *Turcotte and Schubert*, 1982; *Bürgmann et al.*, 1994].

4. Results

[8] Iteratively adjusting D, θ, and T, good fits to the topography are obtained for a relatively narrow range of the fault parameters (Figure 3). Depths of faulting <30 km and >40 km (Figure 3a) produce unacceptable fits to the measured topography. Shallower depths of faulting (<30 km) move the trailing syncline beneath the elevated portion of the scarp. Greater depths of faulting (>40 km) over-predict the topography of the back scarp and move the trailing syncline too far from the scarp face, increasing the upper plate width. Fault-plane dip angles <30° and >35° also produce unacceptable fits to the topography (Figure 3b). Lower fault-plane dips (<30°) under-predict the maximum relief of the scarp and over-estimate the topography of the back scarp and the location of the trailing syncline. Steeper fault-plane dips (>35°) over-estimate the maximum relief of the scarp and predict the trailing syncline too close to the scarp face (under the back scarp). Varying the displacement along the thrust fault changes the amplitude of the predicted topography (Figure 3c). For example, increasing the displacement on the fault by 200 m increases the maximum structural relief by ~120 m (see Figure 3c). The fit does not improve by simultaneously changing a combination of fault parameters while holding another parameter constant. The best fits to the topography across the structure are for T = 35 to 40 km, θ = 30° to 35°, and D = 2.2 km (Figure 3). Changing E from 80 to 40 GPa and ν to 0.2 or 0.3, results in minor changes to the predicted topography.

[9] The predicted topography is influenced by the distribution of relative displacement along the fault. A tapered rather than uniform slip distribution is imposed because it avoids unrealistically large stress concentrations near the fault tips [*Toda et al.*, 1998]. A linear taper within 10 km from the ends of the fault produces the best fit to the topography. Increasing the taper distance results in a decrease in slope of the scarp face and an increase in slope of the back scarp, while slightly increasing the amplitude of the predicted topography, both of which lead to poorer fits to the observed topography. We examined the offset where the fault breaks the surface and cuts the floor of Rameau

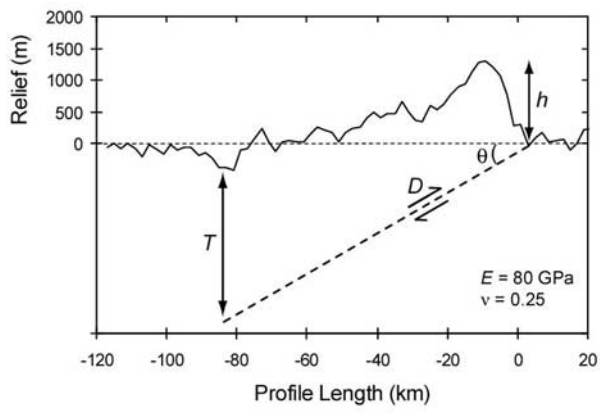

Figure 2. Topographic profile across Discovery Rupes shown with the location of the underlying thrust fault having vertical depth of faulting T, fault-plane dip angle θ, and maximum displacement D. The profile is representative of 6 adjacent profiles spaced at 2 km intervals all of which show the scarp face, back scarp, and a shallow trough. The best model fits are for T = 35–40 km, θ = 30°–35°, and D = 2.2 km. The depth of faulting is not to scale. Vertical exaggeration of topography is 18X.

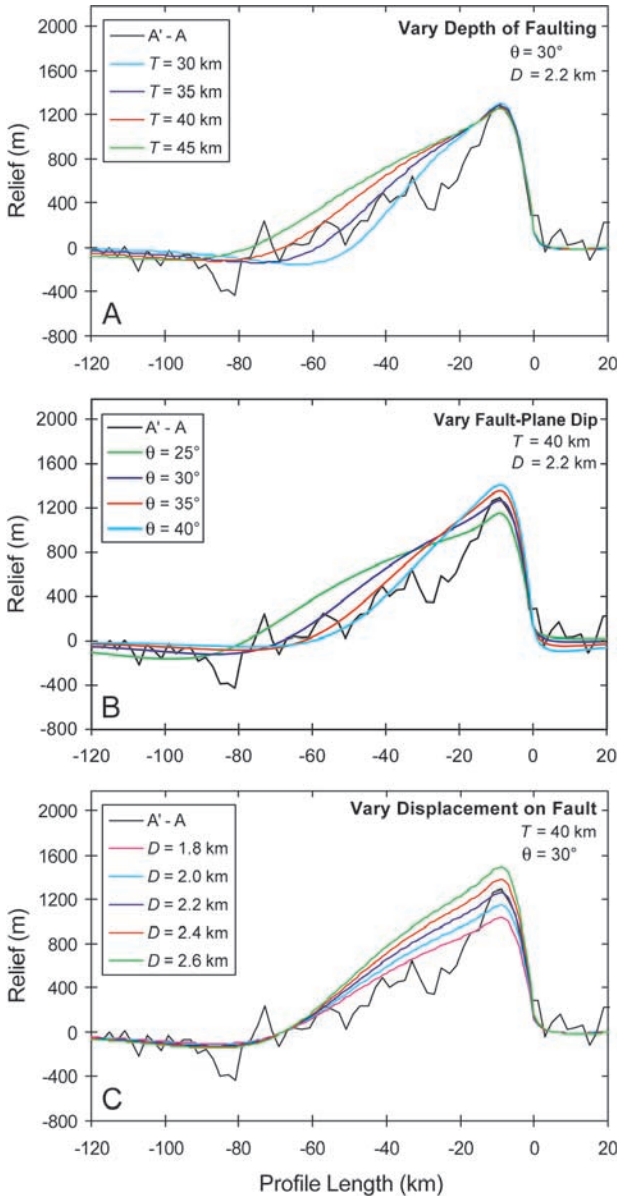

Figure 3. Comparison of predicted structural relief and measured topography across Discovery Rupes. (a) Depth of faulting T is varied while the fault-plane dip θ and displacement D are kept constant. (b) θ is varied while T and D are kept constant. (c) D is varied while T and θ are kept constant. Profile location is shown in Figure 1. Vertical exaggeration is 30X.

crater (Figure 1). The vertical offset appears to be significantly less than the maximum relief suggesting that the observed topography of the scarp primarily developed while the fault was blind (not surface breaking) and propagating up toward the surface, similar to Amenthes Rupes on Mars [*Schultz and Watters*, 2001].

[10] The influence of fault geometry was also investigated. Listric fault geometries were approximated by linear segments with varying dips. The dips of the surface breaking segments were 30° and 15°, and in one case the fault was allowed to flatten into a décollement. None of the listric geometries modeled produce fits to the topographic data as good as the planar geometry. As fault dip shallows with depth, the predicted maximum relief decreases and the fit with the back scarp deteriorates. The most significant deviation from the planar fault geometry is in the predicted syncline. It has a much greater amplitude and is either too close or too far from the scarp face. The poorest overall fit to the topography is obtained where the fault flattens into a décollement. The best approximation to the topography is obtained by a planar fault geometry. If the fault-plane varies in dip with depth, it is unlikely that it changes by more than ±5°, and we infer that more listric fault geometries and décollements are unlikely beneath these mercurian thrust faults.

[11] Estimates of the displacement on the Discovery Rupes thrust fault and other mercurian thrust faults have been made from independent kinematic reconstruction of scarp offsets using measured scarp relief h and assumed values for fault-plane dip θ [*Watters et al.*, 1998, 2000] (Figure 2). The average relief of the section of the scarp being investigated is 1300 m (Figures 2 and 3). The kinematic offset is given by $d = h / \sin\theta$, and for h = 1300 m and θ = 35°, d = 2.27 km. This value agrees well with the displacement (D = 2.2 km) obtained in our mechanical modeling (Figure 3c).

[12] The observed topography across Discovery Rupes is predominantly the result of deformation and has not been significantly altered since the scarp formed. This assumption is supported by high-resolution images of Discovery Rupes (~240 m/pixel) that show no evidence of mass wasting on the scarp face. Erosion from micrometeorite impacts over ~4 Gyr have likely resulted in some modification of the structure. However, estimates of the rate of erosion on the lunar surface from micrometeorites do not exceed 2 m/Gyr [*Crozaz et al.*, 1972; *Gault et al.*, 1972], well within the uncertainty of the topographic data used in this study.

5. Discussion and Conclusions

[13] Little is known about the mechanical or thermal structure of Mercury's lithosphere. Because seismicity reflects stick-slip frictional instability [see *Scholz*, 1998], estimates of the maximum depth of faulting on Mercury provide insights into the thickness of the seismogenic or brittle lithosphere T_s at the time the faults formed. Our results suggest that the Discovery Rupes thrust fault cuts the mercurian lithosphere to a depth of up to 40 km. On Earth's continents, T_s typically coincides with the thickness of the elastic lithosphere T_e (ranging from ~10–40 km), with T_e often less than T_s [*McKenzie and Fairhead*, 1997; *Maggi et al.*, 2000]. Forward modeling of the Amenthes Rupes thrust fault on Mars, a structure analogous to the Discovery Rupes thrust fault [*Watters et al.*, 2000], suggests that the fault extends to a depth of 25 to 30 km [*Schultz and Watters*, 2001]. This is comparable to independently derived estimates of T_e of the martain highlands of ~20 to 30 km using Mars Global Surveyor gravity and topography [*Zuber et al.*, 2000]. If the Discovery Rupes thrust fault extends to a depth of ~40 km and correlates with the extent of the brittle (stick-slip) response of Mercury's lithosphere, it places an upper limit on the elastic thickness. Thus Mercury's elastic lithosphere was about 40 km thick at about 4.0 Gyr ago when the thrust fault formed.

[14] An estimate of T_s from depth of faulting also provides insight into the thermal structure of the mercurian lithosphere at the time the faults formed. The maximum depth of intraplate seismicity on Earth is controlled by the depth to 250° to 450°C isotherm in continental crust and the 600° to 800°C isotherm in oceanic lithosphere [*Chen and Molnar*, 1983; *Wiens and Stein*, 1983]. Although the composition of Mercury's lithosphere is unknown, evidence suggests it is similar to lunar highlands anorthositic crust [cf. *Blewett et al.*, 1997]. We assume the limiting temperature (i.e., frictional stability transition) for Mercury ranges from about 300° to 600°C. The heat flux q through a slab of thickness l is given by

$$q = \frac{k\Delta T}{l} \tag{1}$$

where k is thermal conductivity and ΔT is the temperature difference [see *Turcotte and Schubert*, 1982]. Recent studies show that thermal conductivity varies with pressure and for Earth's

lithosphere ranges from 2 W m^{-1} K^{-1} at the thermal boundary layer (~80 km depth) to over 4 W m^{-1} K^{-1} near the surface [*Hofmeister*, 1999]. Given the reduced acceleration due to gravity, we assume an average k of 3 to 4 W m^{-1} K^{-1} for Mercury's lithosphere [see *Schubert et al.*, 1988; *Nimmo*, 2002], although k may decrease in the heavily fractured near-surface. Using a mean surface temperature of 440 K [*Schubert et al.*, 1988; *Spohn*, 1991], we estimate a heat flux of ~10 to 43 mW m^{-2} for a linear temperature variation, and a paleothermal gradient ~3 to 11 K km^{-1} at the time the thrust fault formed. These may be lower limits if the thermal gradient is non-linear, resulting from a concentration of radiogenic material in Mercury's crust [see *Nimmo*, 2002]. By comparison, Mercury's heat flux at the end of the period of heavy bombardment was less than that of old (>125 Myr) oceanic lithosphere on Earth (~50 mW m^{-2}) [*Sclater et al.*, 1980], but greater than the average present day heat flux on the Moon measured at the Apollo 15 and 17 landing sites (~18 mW m^{-2}) [*Turcotte and Schubert*, 1982]. Our results will be testable when gravity and topographic data are available from MESSENGER [*Solomon et al.*, 2001] and Bepi Colombo.

[15] **Acknowledgments.** We thank Frank Nimmo for helpful discussions and the University College London/Laserscan for the "Gotcha" stereo matching software. This research was supported by grants from National Aeronautics and Space Administration's Planetary Geology and Geophysics Program.

References

Anderson, J. D., R. F. Jurgens, E. L. Lau, and M. A. Slade, Shape and orientation of Mercury from radar ranging data, *Icarus*, *124*, 690–697, 1996.

Bilham, R., and G. King, The morphology of strike-slip faults: Examples from the San Andreas Fault, California, *J. Geophys. Res.*, *94*, 10,204–10,216, 1989.

Blewett, D. T., P. G. Lucey, B. R. Hawke, G. G. Ling, and M. S. Robinson, A comparison of mercurian reflectance and spectral quantities with those of the Moon, *Icarus*, *129*, 217–231, 1997.

Bürgmann, R., D. D. Pollard, and S. J. Martel, Slip distributions on faults: Effects of stress gradients, inelastic deformation, heterogeneous host-rock stiffness, and fault interaction, *J. Struct. Geol.*, *16*, 1675–1690, 1994.

Chen, W., and P. Molnar, Focal depths of intracontinental and intraplate earthquakes and their implications for the thermal and mechanical properties of the lithosphere, *J. Geophys. Res.*, *88*, 4183–4214, 1983.

Cohen, S. C., Numerical models of crustal deformation in seismic zones, *Adv. Geophys.*, *41*, 133–231, 1999.

Cook, A. C., and M. S. Robinson, Mariner 10 stereo image coverage of Mercury, *J. Geophys. Res.*, *105*, 9429–9443, 2000.

Cook, A. C., M. S. Robinson, T. R. Watters, and K. Edwards, Digital elevation model of the Discovery region on Mercury (abstract), *LPSC XXIX*, 1849–1850, 1998.

Cordell, B. M., and R. G. Strom, Global tectonics of Mercury and the Moon, *Phys. Earth Planet. Inter.*, *15*, 146, 1977.

Crozaz, G., R. Drozd, C. M. Hohenberg, H. P. Hoyt, D. Ragan, R. M. Walker, and D. Yuhas, Solar flare and galactic cosmic ray studies of Apollo 14 and 15 samples, *Proceedings of the 3rd Lunar Science Conference, Geochimica et Cosmochimica Acta*, 2917–2931, 1972.

Day, T., A. C. Cook, and J. P. Muller, Automated digital topographic mapping techniques for Mars, *Intern. Arch. Photogrammetry and Rem. Sen.*, *29*, 801–808, 1992.

Gault, D. E., F. Hörz, and J. B. Hartung, Effects of microcratering on the lunar surface, *Proceedings of the 3rd Lunar Science Conference, Geochimica et Cosmochimica Acta*, 2713–2734, 1972.

Hofmeister, A. M., Mantle values of thermal conductivity and the geotherm from phonon lifetimes, *Science*, *283*, 1699–1706, 1999.

King, G. C. P., R. S. Stein, and J. B. Rundle, The growth of geological structures by repeated earthquakes 1, Conceptual framework, *J. Geophys. Res.*, *93*, 13,307–13,318, 1988.

Maggi, A., J. A. Jackson, D. McKenzie, and K. Priestley, Earthquake focal depths, effective elastic thickness, and the strength of the continental lithosphere, *Geology*, *28*, 495–498, 2000.

McKenzie, D., and D. Fairhead, Estimates of the effective elastic thickness of the continental lithosphere from Bouguer and free air gravity anomalies, *J. Geophys. Res.*, *102*, 27,523–27,552, 1997.

Melosh, H. J., and W. B. McKinnon, The tectonics of Mercury, in *Mercury*, edited by F. Vilas, C. R. Chapman, and M. S. Matthews, 374–400, 1988.

Nimmo, F., Constraining the crustal thickness on Mecury from viscous topographic relaxation, *Geophys. Res. Lett.*, *29*, 7-1–7-4, 2002.

Okada, Y., Internal deformation due to shear and tensile faults in a half-space, *Bull. Seismol. Soc. Am.*, *82*, 1018–1040, 1992.

Robinson, M. S., M. E. Davies, T. R. Colvin, and K. E. Edwards, A revised control network for Mercury, *J. Geophys. Res.*, *104*, 30,847–30,852, 1999.

Schenk, P., and H. J. Melosh, Lobate thrust scarps and the thickness of Mercury's lithosphere (abstract), *LPSC XXV*, 1203–1204, 1994.

Schubert, G., M. N. Ross, D. J. Stevenson, T. Spohn, in *Mercury*, edited by F. Vilas, C. R. Chapman, and M. S. Matthews, 429–460, 1988.

Sclater, J. G., C. Jaupart, and D. Galson, The heat flow through oceanic and continental crust and the heat loss of the Earth, *Rev. Geophys. Space Phys.*, *18*, 269–311, 1980.

Scholz, C. H., Earthquakes and friction laws, *Nature*, *391*, 37–42, 1998.

Schultz, R. A., and T. R. Watters, Forward mechanical modeling of the Amenthes Rupes thrust fault on Mars, *Geophys. Res. Lett.*, *28*, 4659–4663, 2001.

Spohn, T., Mantle differentiation and thermal evolution of Mars, *Mercury, and Venus, Icarus*, *90*, 222–236, 1991.

Strom, R. G., N. J. Trask, and J. E. Guest, Tectonism and volcanism on Mercury, *J. Geophys. Res.*, *80*, 2478–2507, 1975.

Solomon, S. C., et al., The MESSENGER Mission to Mercury: Scientific Objectives and Implementation, *Planet. Space Sci.*, *49*, 1445–1465, 2001.

Stein, R. S., G. C. P. King, and J. Lin, Stress triggering of the 1994 M = 6.7 Northridge California, earthquake by its predecessors, *Science*, *265*, 1432–1435, 1994.

Taboada, A., J. C. Bousquet, and H. Philip, Coseismic elastic models of folds above blind thrusts in the Betic Cordilleras (Spain) and evaluation of seismic hazard, *Tectonophysics*, *220*, 223–241, 1993.

Toda, S., R. S. Stein, P. A. Reasenberg, J. H. Dieterich, and A. Yoshida, Stress transferred by the 1995 M_w = 6.9 Kobe, Japan, shock: Effect on aftershocks and future earthquake probabilities, *J. Geophys. Res.*, *103*, 24,543–24,565, 1998.

Turcotte, D. L., and G. Schubert, *Geodynamics*: *Application of Continuum Physics to Geological Problems*, 450 pp., John Wiley, New York, 1982.

Watters, T. R., M. S. Robinson, and A. C. Cook, Topography of lobate scarps on Mercury: New constraints on the planet's contraction, *Geology*, *26*, 991–994, 1998.

Watters, T. R., R. A. Schultz, and M. S. Robinson, Displacement-length relations of thrust faults associated with lobate scarps on Mercury and Mars: Comparison with terrestrial faults, *Geophys. Res. Lett.*, *27*, 3659–3662, 2000.

Watters, T. R., M. S. Robinson, and A. C. Cook, Large-scale lobate scarps in the southern hemisphere of Mercury, *Planet. Space Sci.*, *49*, 1523–1530, 2001.

Wiens, D. A., and S. Stein, Age dependence of oceanic intraplate seismicity and implications for lithospheric evolution, *J. Geophys. Res.*, *88*, 6455–6468, 1983.

Wilkison, S. L., M. S. Robinson, T. R. Watters, and A. C. Cook, Quality assessment of Mariner 10 digital elevation models (abstract), *LPI Contribution No. 1097*, 113–114, 2001.

Zuber, M. T., et al., Internal structure and early thermal evolution of Mars from Mars Global Surveyor topography and gravity, *Science*, *287*, 1788–1793, 2000.

T. R. Watters and A. C. Cook, Center for Earth and Planetary Studies, National Air and Space Museum, Smithsonian Institution, Washington, D.C. 20560-0315, USA. (twatters@nasm.si.edu; tcook@nasm.si.edu)

R. A. Schultz, Geomechanics-Rock Fracture Group, Department of Geological Sciences/172, Mackay School of Mines, University of Nevada, Reno, NV 89557-0138, USA. (schultz@mines.unr.edu)

M. S. Robinson, Department of Geological Sciences, Northwestern University, Evanston, Illinois 60208, USA. (robinson@eros.earth.northwestern.edu)